Reflection Enhanced Compensation of Lossy Traces for Best Eye-Diagram Improvement Using High-Impedance Mismatch

Wei-Da Guo, Feng-Neng Tsai, Guang-Hwa Shiue, and Ruey-Beei Wu, *Senior Member, IEEE*

***Abstract*—As the signal rates increase toward the multigigabit range, the lossy effect of typical transmission lines on the signal quality of printed circuit boards has become a more and more significant issue. This paper introduces the concept of reflection gain resulted from the high-impedance mismatch to improve the eye diagram at the receiving end by inserting the inductance or high-impedance line between the signal trace and matched termination. A systematic design methodology is also proposed here to tell how to resolve the optimal high-impedance elements for the finest compensation efficiency. Moreover, with the optimal inductance, a design formula based on the circuit theory is derived accordingly to estimate the approximate length of high-impedance line and after that, the ultimate performance of this compensation method is also evaluated. Eventually, some experiments are implemented to validate the design technique.**

***Index Terms*—Compensation, eye diagram, high-impedance line, high-impedance mismatch, inductance, lossy transmission line, reflection gain, signal integrity.**

I. Introduction

MODERN technology has been moving toward higher speeds and smaller form factors. Some nonideal effects previously considered to be negligible in printed circuit boards (PCBs) become critical design challenges for meeting the signal/power integrity (SI/PI) and electromagnetic interference (EMI) requirements [1]. Among them, one important effect is the frequency dependent losses of transmission line mainly attributed to the finite conductivity of imperfect conductors and the naturally electric polarization of dielectric materials. It might cause serious intersymbol interference (ISI) problems, leading to the occurrence of poor eye diagram and even false switching of logic gates. This must be taken into account carefully, especially for the digital systems with long-distance data transmission inside.

Manuscript received August 24, 2007; revised October 28, 2007. First published March 31, 2008; last published August 6, 2008 (projected). This work was supported in part by the National Science Council, Taiwan, R.O.C., under Grant NSC 96-2221-E-002-083, in part by the NTU Excellence Research Program under Grant 95R0062-AE00-08, and in part by Inventec Inc. This work was recommendation for publication by Associated Editor J. Tan upon evaluation of the reviewers comments.

W.-D. Guo, F.-N. Tsai, and R.-B. Wu are with the Department of Electrical Engineering and Graduate Institute of Communication Engineering, National Taiwan University, Taipei 10617, Taiwan, R.O.C. (e-mail: rbwu@ew.ee.ntu.edu.tw; f92942062@ntu.edu.tw).

G.-H. Shiue is with the Chung-Yuan Christian University of Science and Technology, Taoyuan 32023, Taiwan, R.O.C.

Color versions of one or more of the figures in this paper are available online at http://ieeexplore.ieee.org.

Digital Object Identifier 10.1109/TADVP.2008.920649

Several works had been presented on how to overcome the excessive signal attenuation effectively. For example, the pre-emphasis/postemphasis technique with the active equalizer at transmitter/receiver was mostly introduced to equalize the high-frequency losses with the direct current (dc) attenuation level [2]–[6]. Some passive equalizers were also developed to get the inverse characteristic of lossy traces over the involved signal bandwidth [7], [8]. The usages of these methods indeed raise the signal quality but will take larger circuit volume, and/or wider PCB area, and extra power consumption as the trade-offs.

Recently, a novel concept adopting the reflection gain for the loss compensation was realized by placing high-impedance elements between the signal line and matched termination [9]. The received eye diagram was improved and the influences of parameter variations were discussed as well. However, the relation between the best achievable compensation efficiency and required high-impedance elements has not been researched yet, and is served as one of major motives to this study.

The paper is organized as follows. In Section II, the compensation principle describes how the reflection gain generated from the high-impedance mismatch helps emphasize the attenuated signal waveform and specifies which frequency range of the output/input voltage ratio response would be best compensated. Then, a systematic design methodology is proposed in Section III to solve how much high-impedance elements should be set versus the length of lossy transmission line and the data rate. Based on the optimal inductance and the circuit theory, a design formula is derived for the approximate length of high-impedance line. With the defined eye-diagram specification, the improvement in the usable length of compensated lossy trace is also evaluated in this section. Section IV compares the proposed design with the measurement results to validate the idea further. At last, some conclusions are drawn in Section V.

II. Compensation Principle

A typical transmission line system is depicted in Fig. 1(a) for example, which mainly consists of a transmitter, a receiver, and a single-ended microstrip line in between. In practice, the transmitter is equivalent to a voltage source followed by a serial resistor, while the receiver is of very high input impedance. The voltages of the source V_S and the node V_O are then related by

$$V_O(f) = \left(\frac{Z_0}{Z_0 + R_S} \cdot \frac{H(f) \cdot [1 + \Gamma_L(f)]}{1 - H^2(f) \cdot \Gamma_S(f) \cdot \Gamma_L(f)}\right) \cdot V_S(f) \quad (1)$$

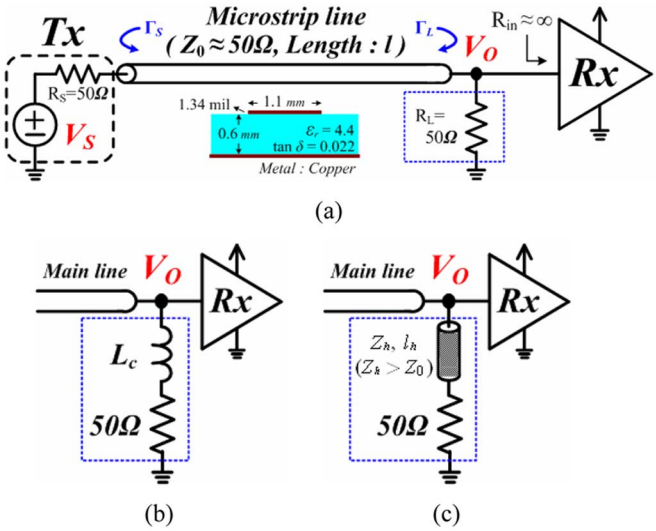

Fig. 1. Typical transmission line system with (a) matched load, (b) matched load in series with an inductance, and (c) matched load in series with a high impedance line section. Cross section of the transmission line is shown in inset.

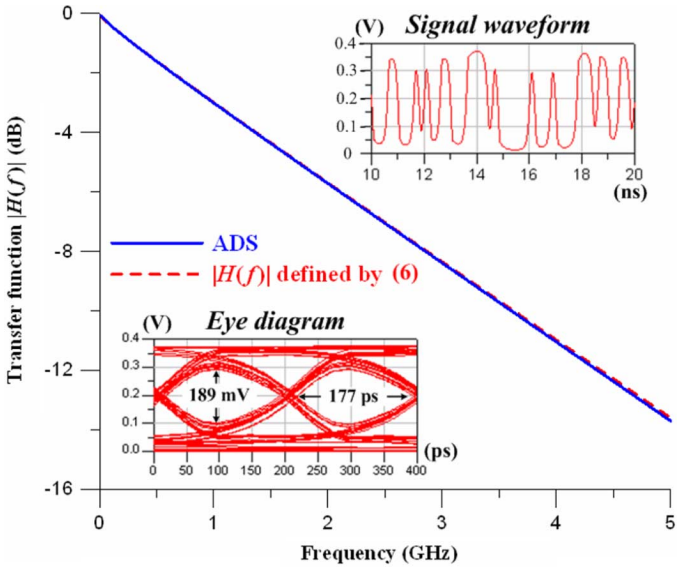

Fig. 2. Transfer function of 30-in lossy line in Fig. 1(a) as well, as fractional signal waveform and resultant eye diagram at node V_O.

where $H(f)$ represents the transfer function of the lossy transmission line, as well as $\Gamma_S(f)$ and $\Gamma_L(f)$ means the reflection coefficients in the transmitted and received ends, respectively. Note that the frequency dependency of the characteristic impedance Z_0 is ignored here with the assumption of low-loss line [10].

In common cases, the trace is terminated with nearly matched resistances in both ends for avoiding multiple reflections. As a result, (1) is simplified to be

$$V_O(f) \approx H(f) \cdot \frac{V_S(f)}{2}. \tag{2}$$

When a high-impedance element is further inserted into the load termination, as illustrated in Fig. 1(b) or (c), a positive reflection owing to the impedance mismatch will take place at the very point that the lossy line and the load termination are connected [9]. Since $\Gamma_S(f)$ is still close to zero, the voltage relation between the V_S and V_O can be approximated by

$$V_O(f) \approx H(f) \cdot [1 + \Gamma_L(f)] \cdot \frac{V_S(f)}{2}. \tag{3}$$

This implies that the impedance mismatch can possibly boost the attenuated signal voltage. However, owing to the frequency-dependent nature of the reflection gain $[1+\Gamma_L(f)]$, how to find out the optimum high-impedance element motivates our study for the best compensation efficiency.

To investigate the design concept, the serious effect of transmission-line losses has to be discussed first. The input data pattern adopts the pseudo-random bit sequence (PRBS) with data rate of 5 Gbps and voltage amplitude of 0.8 V. The rising edge of the signals is fixed at one quarter of an individual bit period. From the simulation by Advanced Design System (ADS) [11], the transfer function of 30-in-long line, the sample waveform of received signal, and the resultant eye diagram at the node V_O are all displayed in Fig. 2. The excessive high-frequency attenuation indeed slacks off the transition edge of digital signal and induces nonnegligible ISI problem. The eye height is reduced from 400 to 189 mV, while the eye width is narrowed from 200 to 177 ps. It is clear that the noise margin degrades and the maximal frequency range in which the system can operate will be influenced as well.

After introducing the load termination of Fig. 1(b), the effect of the inserted inductance on the output eye diagram is plotted in Fig. 3(a). As the inductance value increases, it initially is capable of enlarging the maximum eye opening. However, the improvement reaches its maximum at certain value, say 8 nH in the present case, and then drops slightly due to too much reflection. Further referring to Fig. 3(b), because of unavoidable voltage divided effect induced by the source and load termination resistances, here we define the voltage transmission coefficients as

$$|V_T(f)| \equiv |2 \cdot V_O(f)/V_S(f)|. \tag{4}$$

After calculating the values by (4) under $L_c = 0, 2.5, 5, 8$, and 10 nH, it is observed that the reflection gain $|1 + \Gamma_L(f)|$ enhances with inductance and frequency, but will reach at most 6 dB. Near the best inductance of 8 nH, the combination of the $|H(f)|$ and the $|1 + \Gamma_L(f)|$ can give a quite flat response, i.e., an equalization effect, over a certain frequency range. As shown in the inset of Fig. 3(b), this occurrence makes all signal transitions in nearly full swing, thus attaining the best eye-diagram improvement. For even larger inductance, e.g., $L_c = 10$ nH, the curve shows an evident peak at about 1 GHz. It results in loss unbalance so that an overcompensation condition happens.

The analysis has been made for the transmission line with other trace length l. Though not presented here, they all lead to the same observation that the maximally flat voltage transmission coefficient versus frequency can achieve the best eye-diagram compensation. It is worthwhile to consider two extreme cases that the transmission line has only conductor skin-effect loss or dielectric loss. For the latter case, the dielectric loss is proportional to frequency f. The eye-diagram can be shown to keep the same if the bit period and inductance is normalized with the trace length l. Similar argument holds for the former case in which the loss is proportional to $\sqrt{f}$ and the normalization should be taken with l^2.

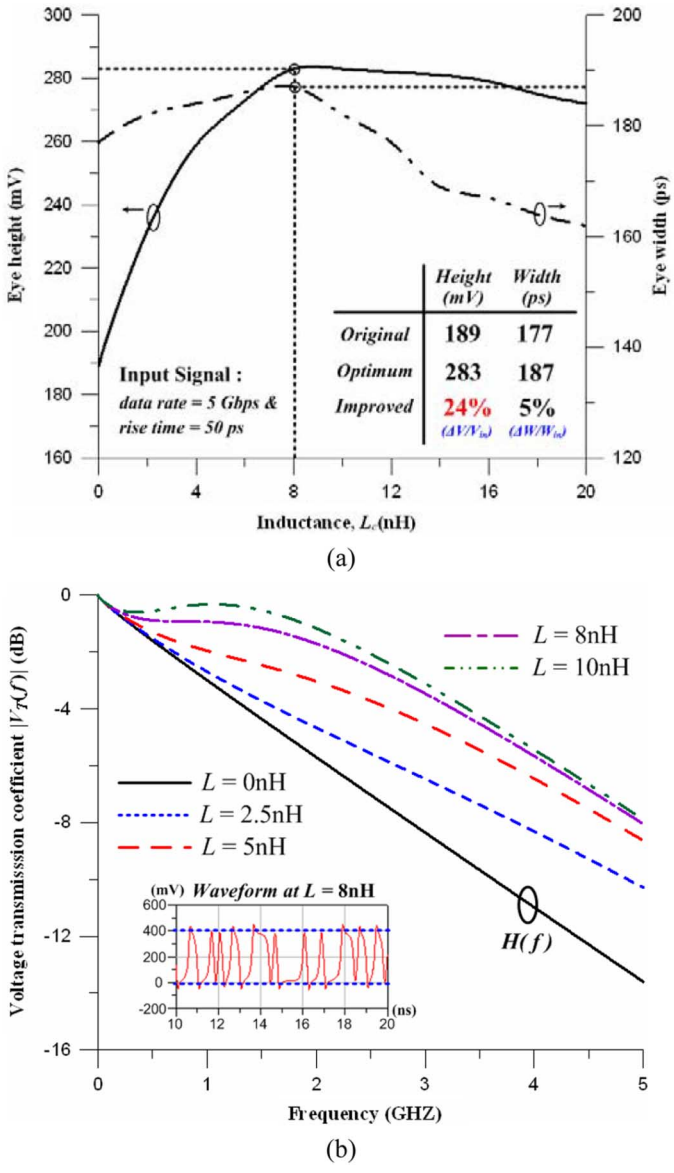

Fig. 3. Comparison of compensation efficiency with inserted inductance as a parameter. (a) Eye-diagram performance versus inserted inductance and (b) voltage transmission coefficient versus frequency with inserted inductance as a parameter. Eye-diagram improvement and a simulated bit sequence of system with best inductance are shown in insets.

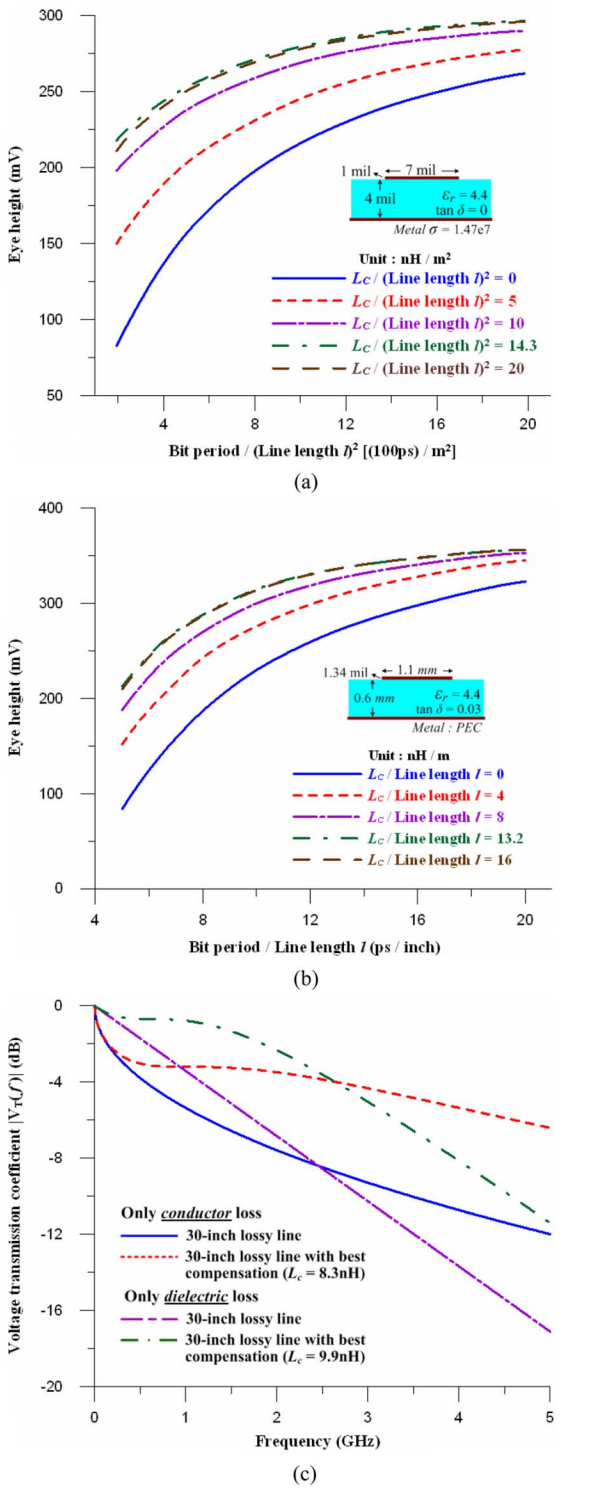

Fig. 4. With inductance-inserted load termination, comparison of compensation efficiency for transmission line that has (a) conductor loss only, (b) dielectric loss only, and (c) resultant voltage transmission coefficient versus frequency for optimum inductance selection in (a) and (b). Cross sections of transmission line used in simulation are shown in insets.

Fig. 4(a) and (b) shows the eye openings versus various bit periods and inductance values for both extreme cases. The best compensation condition happens at $L_c/l^2 = 14.3\,\mathrm{nH/m^2}$ and $L_c/l = 13.2\,\mathrm{nH/m}$, respectively. Assuming a trace length of 30 in, the best inductance happens at 8.3 and 9.9 nH, respectively, for the two cases. Fig. 4(c) shows the voltage transmission coefficient versus the frequency. It is demonstrated that the criterion of maximally flat response for the best compensation efficiency remains the same.

Besides, it is noted that the optimum inductance is less dependent on the specification of signal data rate, which affects the frequency range of the voltage distribution to sense the lossy effect. Nevertheless, the trace length is more critical in determining the shape of the initial $|V_T(f)|$. If the length becomes longer, a larger inductance is needed to raise $|V_T(f)|$ to a flat level. Hence, the design of this compensation technique should greatly relate to the degree of lossy effect, while the signal data rate merely decides the resultant eye diagram. Through the comparison of the eye-diagram parameters both in Fig. 4(a) and (b),

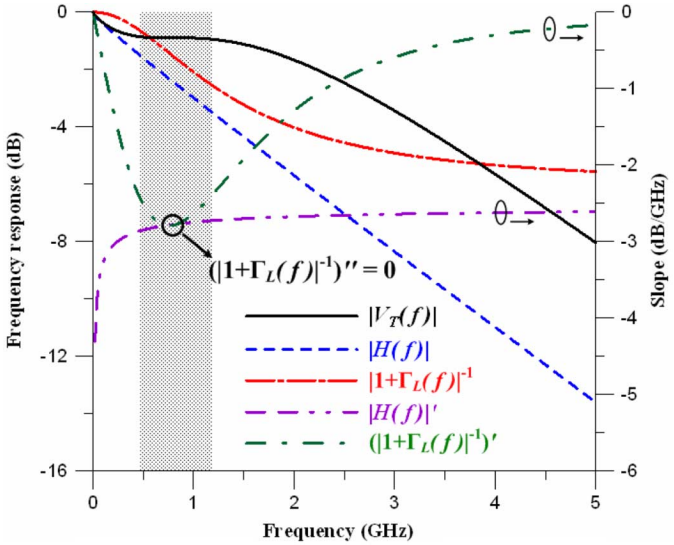

Fig. 5. Frequency responses of $|V_T(f)|$, $|H(f)|$, and $|1+\Gamma_L(f)|^{-1}$ under $L = 8$ nH and their associated slopes.

one thing also worth mentioning that the more the high-frequency components of digital signal or the trace losses, the worse the original and so the well-compensated system performances will be.

In modern technology, the system performance at the transmitted end has also gained much more attention than before. The reflection gain indeed compensates the lossy effect of transmission line, however, the induced reflected wave that moves backward to the voltage source will be possibly harmful to the operation of transmitter circuit and thus needs to be considered carefully in this compensation design.

III. Design Methodology

A. Inductance Insertion

In order to determine the optimum inductance, the prime work is to investigate the relation between the $|H(f)|$ and the $|1+\Gamma_L(f)|$ so as to meet the well-compensated $|V_T(f)|$. The separate frequency responses associated with the well-compensated $|V_T(f)|$ in Fig. 3(b) are all shown in Fig. 5. Note that the $|1+\Gamma_L(f)|$ is replaced with its reciprocal and the $|V_T(f)|$ in dB can thus be given by

$$20\log|V_T(f)| = 20\log|H(f)| - 20\log|1+\Gamma_L(f)|^{-1}. \quad (5)$$

The curves of the $|H(f)|$ and the $|1+\Gamma_L(f)|^{-1}$ under $L = 8$ nH are apparently parallel to each other within the shaded region in which the well-compensated $|V_T(f)|$ is rather flat. It is thus required that the slopes of the two responses, $|H(f)|'$ and $(|1+\Gamma_L(f)|^{-1})'$, be locally identical near the frequency where the second derivative of $|1+\Gamma_L(f)|^{-1}$ is zero.

Once the numerical expressions for the slopes of the two responses are available, the optimum inductance can be obtained accordingly. In general, the transfer function $|H(f)|$ of the lossy transmission line takes the form of

$$|H(f)| = 20*\log(e^{-\alpha l})\ (\text{dB}) \quad (6)$$

where α is the attenuation constant and l is the line length. On the other hand, the reciprocal of the reflection gain $|1+\Gamma_L(f)|^{-1}$ due to the inserted inductance can be given by

$$|1+\Gamma_L(f)|^{-1} = -10*\log\left(\frac{4+4p^2}{4+p^2}\right) \quad (7)$$

where $p = 2\pi f * L_c/Z_0$. After setting the second derivative of (7) to be zero, it is deduced that the inflection point of $|1+\Gamma_L(f)|^{-1}$ will locate at $p \approx 0.77$, namely

$$2\pi f \cdot L_c \approx 0.77*50 = 38.5. \quad (8)$$

Equalizing the differentiation of (6) and (7) yields

$$\frac{d\alpha}{df} * l = \frac{3p^2}{f[1+p^2][4+p^2]}. \quad (9)$$

Given the attenuation constant α, f can be found from (9) since $p = 0.77$, and then the desired optimum inductance L_c from (8).

To be more specific, consider the low-loss transmission line and assume the value α given by

$$\alpha \approx 0.5*(R*\sqrt{C/L} + G*\sqrt{L/C}) \quad (10)$$

where

$$R \approx \sqrt{\rho\pi\mu f}/\text{W} \quad \text{and} \quad G \approx 2\pi f * C * \tan\delta \quad (11)$$

where W is the width of the transmission line, and the per-unit-length inductance L and capacitance C can be computed by the 2-D method of moments [10], [12]. It is worth noting that the thus characterized $|H(f)|$ is in good agreement with that from the ADS simulation, as compared in Fig. 2.

By (9) and (10), the optimum inductance satisfies

$$\left(\frac{1}{Z_0}\cdot\frac{dR}{df} + Z_0\cdot\frac{dG}{df}\right) * l = \frac{3.97}{Z_0}\cdot L_c, \quad (12)$$

where $Z_0 = \sqrt{L/C} \approx 50$. For a 30-in transmission line of Fig. 1(a), the optimum inductance equals 7.96 nH, which is close to that of Fig. 3.

By the way, if the trace has dominant conductor or dielectric loss, it is easy to infer that the inductance L_c will be almost directly proportional to $l^2(\text{G} \approx 0)$ or $l(\text{R} \approx 0)$.

B. High-Impedance Transmission Line Insertion

Alternatively, a section of high-impedance transmission line is also capable of accomplishing the same signal-emphasis effect. The objective is to design for the best transmission line section, To simplify this study, the relatively short high-impedance line is considered to be lossless and the associated reflection gain $|1+\Gamma_h(f)|$ is described by

$$|1+\Gamma_h(f)| = 10*\log\left(\frac{4Z_h^2Z_0^2 + 4Z_h^4\tan^2(\beta_h l_h)}{4Z_h^2Z_0^2 + (Z_h^2+Z_0^2)^2\tan^2(\beta_h l_h)}\right)(\text{dB}) \quad (13)$$

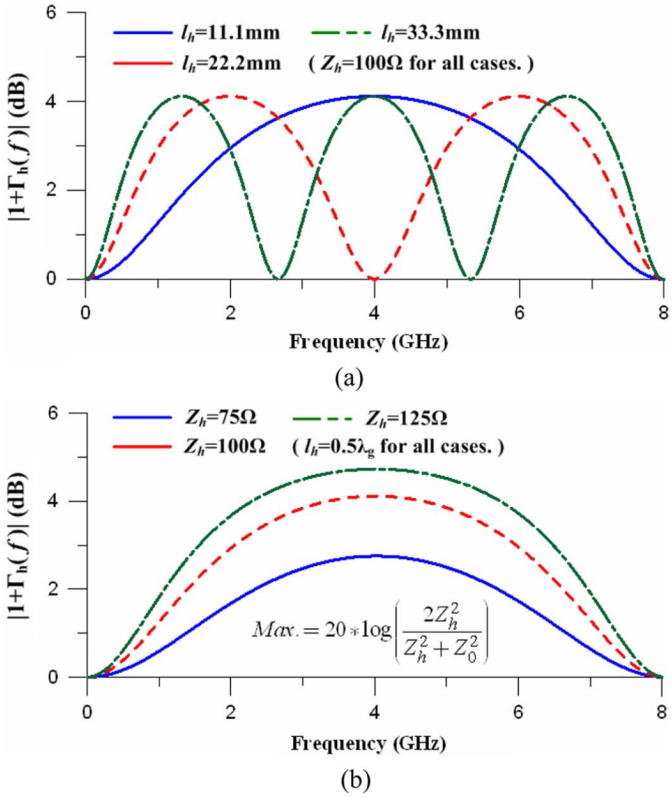

Fig. 6. Comparison of reflection gain $|1+\Gamma_h(f)|$ for high impedance transmission line insertion with (a) different line length and (b) different impedance as a parameter.

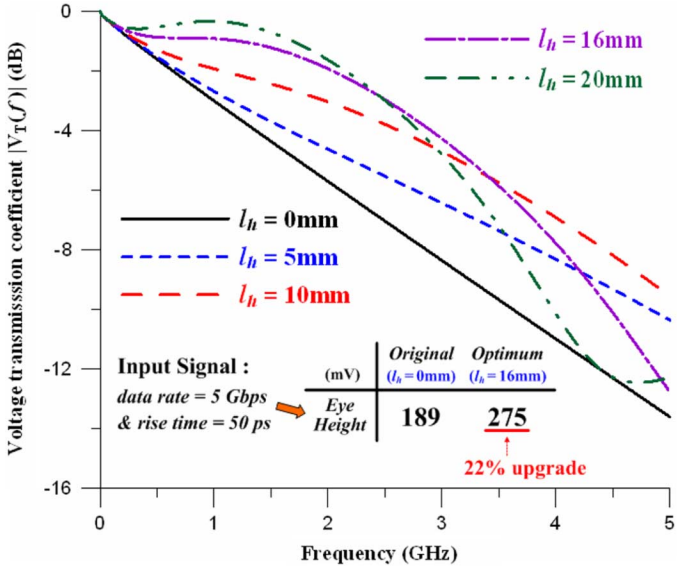

Fig. 7. Comparisons of compensation efficiency with high-impedance line length as a parameter. Eye diagram improvement with optimal line length is shown in inset.

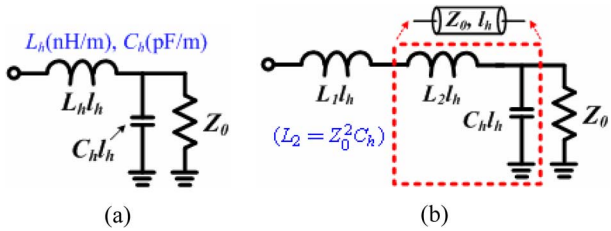

Fig. 8. (a) Equivalent circuits for high-impedance line inserted load termination depicted in Fig. 1(c). ($Z_0 = 50\ \Omega$) and (b) definition of excess inductance L_1.

where Z_h, β_h, and l_h denote the characteristic impedance, the propagation constant, and the length of the inserted line section, respectively.

As the Z_0 is still fixed to be 50 Ω, it can be observed in Fig. 6 that $|1+\Gamma_h(f)|$ varies periodically with frequency and its maximum, which is decided by the corresponding Z_h, will appear at frequencies when the inserted line section equals odd number times of the quarter wavelength. These also imply that $|1+\Gamma_h(f)|^{-1}$ will possibly have more than one inflection point over the involved frequency range. Because the flat response of the well-compensated $|V_T(f)|$ in Fig. 3(b) is situated at lower frequencies, it is better to choose the first inflection point in the design.

A similar procedure can be employed to design for the required length of high-impedance line. For example, consider that the high-impedance line is of $Z_h = 100\ \Omega$. The first inflection point is numerically deduced to locate at where $\beta_h * l_h = 0.41$. If the same lossy trace shown in Fig. 2 is employed, the optimal length can be found to be at 16.1 mm, which is consistent to the simulation results in Fig. 7. Moreover, owing to the inherent periodicity of $|1+\Gamma_h(f)|$, the best eye opening here is slightly smaller than that of the inductance-insertion method in Fig. 3(a).

Although $|1+\Gamma_h(f)|$ can be analytically derived, its complicated expression prohibits the derivation of simple design formulae like (8) and (12). Instead, an alternative approach for the length estimation is built up to facilitate the compensation design. First, the high-impedance line section is modeled by a simple lumped circuit using quasi-static approximation. Consequently, the load termination of Fig. 1(c) is supposed to be equivalent to the circuit form, as depicted in Fig. 8(a). Then, the lumped inductance is split into two elements, one of which being $(Z_0^2 C_h) l_h$. Fig. 8(b) displays that the high-impedance line segment actually can be regarded as a lumped inductance in series with a 50-Ω transmission line of delay time $l_h/\sqrt{L_2 C_h}$. The excess inductance is thus obtained by [13]

$$L_e = L_1 l_h = \left(L_h - Z_0^2 C_h\right) * l_h = \left(Z_h - \frac{Z_0^2}{Z_h}\right) * \frac{l_h}{v_h}(\text{nH}) \tag{14}$$

where v_h is the wave velocity of high-impedance line. Equating it to the optimum inductance given in (12) can give an approximate solution to the optimum line length.

To demonstrate this, the calculated results of three different samples are all shown in Table I. It can be found that the values deviate from the optimal ones but the relative errors are always kept to be about -13%. The approximation would be better if only the nearly constant error is subtracted from the calculated

TABLE I
COMPARISONS BETWEEN OPTIMAL LENGTHS AND CALCULATED RESULTS BY (14) OF THE HIGH-IMPEDANCE LINE

	20 inch (L_c=5.25nH)	30 inch (L_c=7.96nH)	30 inch (L_c=7.96nH)
Line property	Z_h=100Ω; ε_e=2.91	Z_h=100Ω; ε_e=2.91	Z_h=120Ω; ε_e=2.81
Optimal	10.7mm	16.1mm	12.6mm
Calculated	12.3mm	18.5mm	14.4mm
Relative error (%)	**-13%**	**-13%**	**-12.5%**

lengths. After the adjustment, the estimation method is helpful in predicting the required length of high-impedance line.

C. Effect of System Parameter Variation

Because of real manufacturing constraints, a range of impedance variation caused by unavoidable parameter variations is always reserved for the design of high-speed system interconnects. Typically, the variation is restricted to be within $\pm 10\%$ to maintain good signal quality. It is imperious to investigate how much effect of this impedance variation on the compensation design.

Reconsidering the transmission line system in Fig. 1(a), instead, the trace width is reassigned to be 0.9 mm ($Z_0 \approx 55\Omega$) or 1.3 mm ($Z_0 \approx 45\Omega$). If the termination resistors vary accordingly so that the system is still under well-matched situation, the proposed design methodology can still be employed and the resolved the optimum inductance will be 8.9 and 7.2 nH, respectively, almost directly proportional to the impedance variation.

On the other hand, when the termination resistors are fixed at 50 Ω, the eye-diagram performance versus the inductance value can be repeated to exploit the best compensation. Although not shown here, the results indicate that the optimum inductance for the eye-diagram compensation vary by $\pm 2.5\%$, versus a change of $\pm 10\%$ in Z_0. Hence, the present design methodology is still applicable to obtain the required high-impedance element with tolerable error, while the selection of reference impedance Z_0 in the calculation of $\Gamma_L(f)$ should be based on the value of termination resistance.

D. Maximal Usable Length

Furthermore, a standard eye mask is often defined and then employed to evaluate if the interconnects routed among the chip modules are workable for the transmitting signals with certain specification. This indicates that there is an upper limit on the usable length of lossy transmission line. Despite the compensation method can help improve the system performance, an ultimate will exist because the well-compensated $|V_T(f)|$ of Fig. 3(b) is still "lossy."

Intuitively, the usable length for the lossy trace with or without the compensation scheme will not only be relevant to the defined eye mask but also be sensitive to the variations in the signal specification and the line geometry. On the basis of the above discussion, the signal with more high-frequency components or the trace with more losses will lead to the worse eye-diagram performance no matter whether the compensation method is introduced.

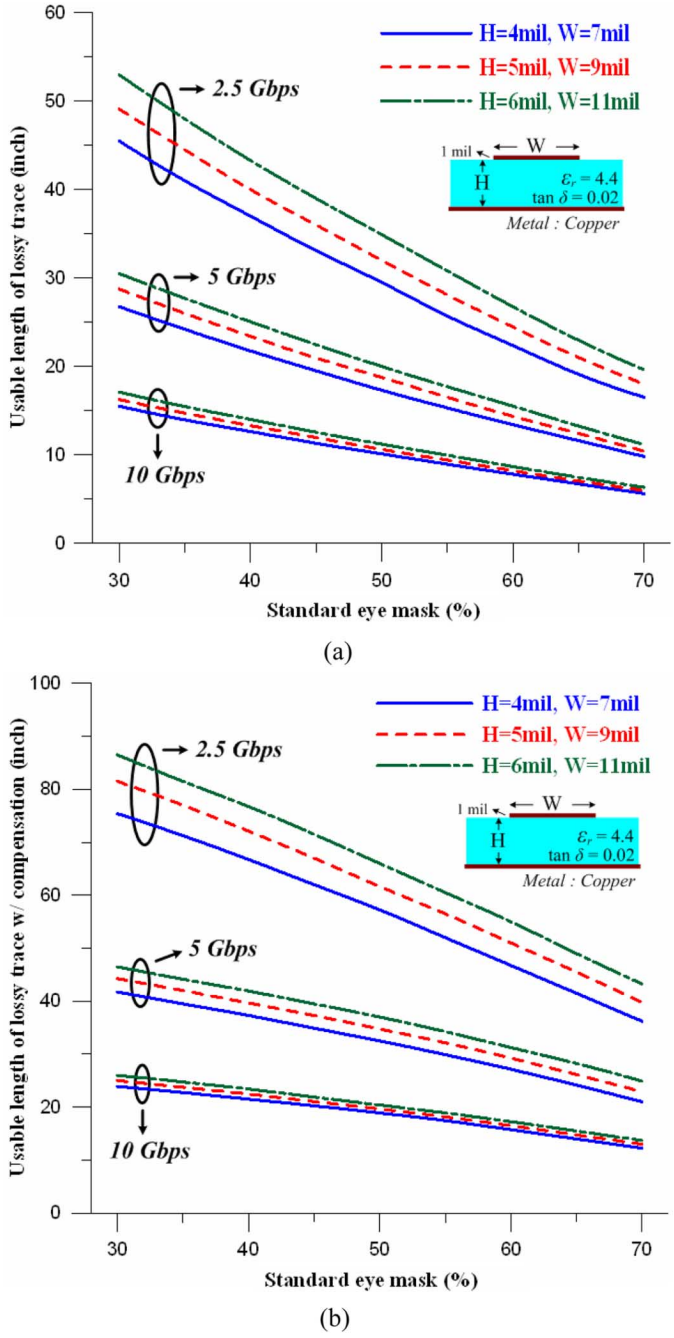

Fig. 9. Curves of maximal usable length of lossy trace with signal date rate as a parameter in cases of (a) without and (b) with inductance-insertion compensation. Cross section of line geometries in PCB scale is shown in inset.

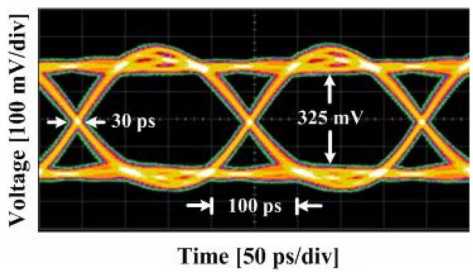

Fig. 10. Measured eye diagram without board under test.

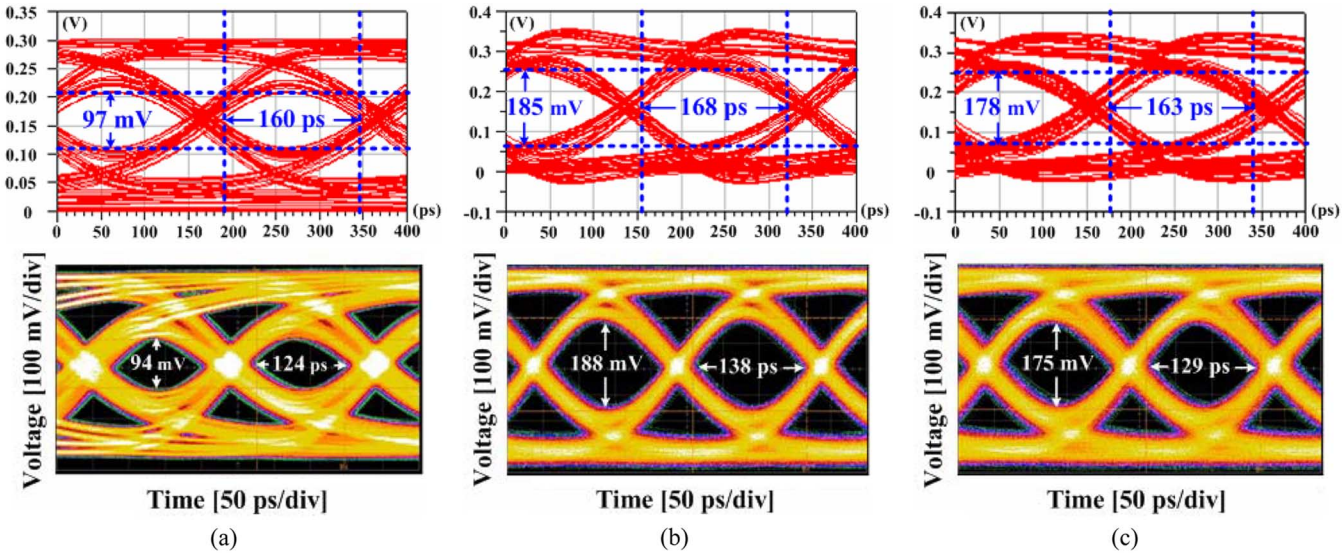

Fig. 11. Comparisons between simulated and measured eye diagrams of lossy traces with three kinds of load terminations shown in Fig. 1: (a) original matched termination, (b) inductance enhancement, and (c) high-impedance line enhancement. (Upper eye: Simulation. Lower eye: Measurement).

Concerning the 50-Ω microstrip lines in PCB scale, two design graphs evaluating the usable lengths for lossy traces with and without the inserted inductance are constructed numerically and given in Fig. 9. The percent eye mask here is expressed in terms of the ratio of the eye height to the 400-mV input voltage. Both graphs show that the maximal usable lengths vary almost linearly with the percent eye mask, the signal rate, and the physical dimension of transmission line. Therefore, exploiting the linear interpolation is able to compute the usable lengths associated with other parameters surrounded by the data curves of Fig. 9. With rapid increase of system operating frequency, it should be noted that the usable length of lossy transmission line will get smaller and smaller. This must be kept in mind more cautiously in the prelayout of high-speed digital system.

IV. Experimental Verification

A test board whose geometry is consistent with that of Fig. 1 was fabricated for verification of the compensation methods. The eye diagrams at the node V_O were measured on Agilent 54855 A digital signal oscilloscope, while the pseudorandom bit sequence with data rate of 5 Gbps, rise time of 50 ps, and voltage amplitude of 0.8 V was launched from Anritsu MP1763C pulse pattern generator. Between the test board and instruments there need coaxial cables for connections. Before the bit sequence transmits through the designed structure, it can be found in Fig. 10 that the measured eye diagram has suffered from degradation due to the existing cable loss and the inherent nonideal effects in the pulse pattern generator. The signal settings in ADS environment necessitate some modifications accordingly to proceed with accurate eye-diagram simulation.

When the length of the lossy traces is arranged to be 38 in, applying the proposed design procedure yields the optimum high-impedance element of 10 nH inductance or 20 mm length of 100-Ω high-impedance line. The simulated and measured eye diagrams of the lossy traces with three kinds of load terminations are demonstrated in Fig. 11. By subtracting the internal jitter of 30 ps shown in Fig. 10, it is clear to see that the comparisons are in good agreement. Then, the exactitude of the compensation methods can be verified.

V. Conclusion

The concept of reflection gain resulted from the high-impedance mismatch has been successfully introduced to alleviate the degraded eye-diagram performance of a lossy transmission line. The parametric analyses of inductance in the inductance inserted load termination also state that the best compensation efficiency occurs only when the compensated voltage transmission coefficient appears maximally flat behavior over a certain frequency range. Following that, a systematic design methodology is proposed to quickly solve the optimal inductance or length of high-impedance line inserted into the conventional matched termination.

For the inductance inserted compensation, a simple expression has been derived to give the optimum inductance design. For the design of high-impedance line, the optimum length can be obtained approximately using a quasi-static equivalent circuit followed by an empirical correction factor. Two design graphs are constructed as well to evaluate the maximal usable length of PCB-scale transmission line that is under compensation or not. Finally, good agreement between the simulated and measured eye diagrams is demonstrated, which validates the correctness and practicability of the compensation methods.

References

[1] S. H. Hall, G. W. Hall, and J. A. McCall, *High-Speed Digital System Design, a Handbook of Interconnect Theory and Design Practices*. New York: Wiley, 2000, ch. 2–5.

[2] W. J. Dally and J. Poulton, "Transmitter equalization for 4 Gbps signaling," *IEEE Micro*, vol. 17, no. 1, pp. 48–56, Jan./Feb. 1997.

[3] M.-J. E. Lee, W. Dally, and P. Chiang, "A 90 mw 4 Gb/s equalized I/O circuit with input offset cancellation," in *ISSCC Dig. Tech. Papers*, Feb. 2000, vol. 43, pp. 252–253.

[4] K. Tanake, M. Fukaishi, M. Takeuchi, N. Yoshida, K. Minami, K. Yamaguchi, H. Uchida, Y. Morishita, T. Sakamoto, T. Kaneko, M. Soda, M. Kurisu, and T. Saeki, "A 100-gb/s transceiver with GND-VDD common-mode receiver and flexible multi-channel aligner," in *IEEE Int. Solid-State Circuits Conf. Dig. Tech. Papers*, Feb. 2002, vol. 1, pp. 264–265.

[5] J. N. Babanezhad, "A 3.3-V analog adaptive line-equalizer for fast ethernet data connection," in *Proc. IEEE Custom Integrated Circuit Conf.*, May 1998, pp. 343–346.

[6] Y. Kudoh, M. Fukaishi, and M. Mizuno, "A 0.13-μm CMOS 5-gb/s 10-m 28AWG cable transceiver with no-feedback-loop continuous-time post-equalizer," *IEEE J. Solid-State Circuits*, vol. 38, no. 5, pp. 741–746, May. 2003.

[7] E. P. Sayre, J. H. Chen, and R. Elco, "Design of gigabit copper fibre channel equalized cabling," in *Digital Commun. Syst. Design Conf.*, Jan. 1998 [Online]. Available: http://www.nesa.com

[8] W. Humann, "Compensation of transmission line loss for gbit/s test on ates," in *Proc. IEEE Int. Test Conf.*, Baltimore,, MD, Oct. 2002, pp. 430–437.

[9] K. Yamagishi and S. Saito, "Methods of eye-pattern window improvement using reflections caused by impedance mismatch: Post-Emphasis technique," *IEEE 14th Topical Meeting Elect. Perform. Electron. Packag.*, pp. 209–212, Oct. 2005.

[10] N. N. Rao, *Elements of Engineering Electromagnetics*, 5th Edition ed. Englewood Cliffs, NJ: Prentice Hall, 2000, chap. 7.

[11] Advanced Design System. ver. 2005A, Agilent Inc. [Online]. Available: http://www.agilent.com

[12] D. B. Davidson, *Computational Electromagnetics For RF and Microwave Engineering*. Cambridge, U.K.: Cambridge Univ. Press, 2005, ch. 7–8.

[13] C. L. Wang and R. B. Wu, "Modeling and design for electrical performance of wide-band flip-chip transition," *IEEE Trans. Adv. Packag.*, vol. 26, no. 4, pp. 385–391, Nov. 2003.

Wei-Da Guo was born in Taoyuan, Taiwan, R.O.C., on September 25, 1981. He received the B.S. degree in communication engineering from National Chiao-Tung University, Hsinchu, Taiwan, R.O.C., in 2003, and is currently working toward the Ph.D. degree in communication engineering at National Taiwan University, Taipei, Taiwan, R.O.C.

His research topics include computational electromagnetics, signal/power integrity (SI/PI) and electromagnetic interference/compatibility (EMI/EMC) issues in the design of high-speed digital systems.

Feng-Neng Tsai was born in Kaohsiung, Taiwan, R.O.C., in 1979. He received the B.S. degrees in electrical engineering from Cheng-Hsiu University of Science and Technology, Kaohsiung, Taiwan, R.O.C., in 2000, and the M.S. degree in communication engineering from National Taiwan University, Taipei, Taiwan, R.O.C., in 2007.

His researches of interest contain signal integrity (SI) issues in the design of high-speed digital systems, and WLAN system circuit design.

Guang-Hwa Shiue was born in Tainan, Taiwan, R.O.C., in 1969. He received the M.S. degree in electrical communication engineering from National Taiwan University of Science and Technology, Taipei, Taiwan, R.O.C., in 1997, and the Ph.D. degree in communication engineering from National Taiwan University, Taipei, Taiwan, R.O.C., in 2006.

He is currently an Assistant Professor with the Electronics Department, Chung-Yuan Christian University of Science and Technology, Taoyuan, Taiwan 32023, R.O.C. His areas of interest include numerical techniques in electromagnetics, microwave planar circuits, signal/power integrity (SI/PI) and electromagnetic interference/compatibility (EMI/EMC) for high-speed digital systems, and electrical characterization of system-in-package.

Ruey-Beei Wu (M'91–SM'97) received the B.S.E.E. and Ph.D. degrees from National Taiwan University, Taipei, Taiwan, in 1979 and 1985, respectively.

In 1982, he joined the faculty of the Department of Electrical Engineering, National Taiwan University, where he is currently a Professor and the Department Chair. He is also with the Graduate Institute of Communications Engineering established in 1997. From March 1986 to February 1987, he was a Visiting Scholar at the IBM East Fishkill Facility, NY. From August 1994 to July 1995, he was with the Electrical Engineering Department, University of California, Los Angeles. He was also appointed Director of the National Center for High-Performance Computing (1998–2000) and has served as Director of Planning and Evaluation Division since November 2002, both under the National Science Council. His areas of interest include computational electromagnetics, microwave and millimeter wave planar circuits, transmission line and waveguide discontinuities, and interconnection modeling for computer packaging.